Research paper

CARINA: A near-Earth D-type asteroid sample return mission

Tânia M. Ribeiro [a],[*], Andrea D'Ambrosio [b], Guillermo J. Dominguez Calabuig [c], Dimitrios Athanasopoulos [d], Helena Bates [e], Clemens Riegler [f], Oriane Gassot [g], Selina-Barbara Gerig [h], Juan L. Gómez-González [i], Nikolaus Huber [j], Ragnar Seton [k], Tiago E.C. Magalhães [a]

[a] *Instituto de Física de Materiais Avançados, Nanotecnologia e Fotónica, Departamento de Física e Astronomia, Faculdade de Ciências, Universidade do Porto, Rua do Campo Alegre s/n, 4169-007 Porto, Portugal*
[b] *Department of Systems and Industrial Engineering, University of Arizona, 1127 E. James E. Rogers Way, Tucson, AZ 85721-0020, United States of America*
[c] *German Aerospace Center (DLR), Germany*
[d] *Section of Astrophysics, Astronomy and Mechanics, Department of Physics, National and Kapodistrian University of Athens, Zografos GR 15784, Athens, Greece*
[e] *Planetary Materials Group, Natural History Museum, London, SW7 5BD, UK*
[f] *Computer Science VIII, Space Engineering, JMU Würzburg, 97074 Würzburg, Germany*
[g] *Université Grenoble Alpes, IPAG, CNRS, 38000, Grenoble, France*
[h] *Physikalisches Institut, University of Bern, Sidlerstrasse 5, 3012, Bern, Switzerland*
[i] *Institute for Research in Technology, ICAI, Comillas Pontifical University, c/ Sta. Cruz de Marcenado, 26, 28015, Madrid, Spain*
[j] *Department of Information Technology, Uppsala University, Sweden*
[k] *Ångström Space Technology Centre, Div. of Microsystems Technology, Dept. of Material Science and Engineering, Uppsala University, Lägerhyddsvägen 1, 752 37, Uppsala, Sweden*

ARTICLE INFO

ABSTRACT

D-type asteroids are among the most primitive small bodies of the solar system. Believed to be formed in the outer solar system, a minor fraction of these faint objects can be found in the near-Earth region. Some were suspected to be extinct comets disguised as asteroids. If D-type near-Earth asteroids could represent extinct comets, they would offer us a unique opportunity to investigate the relationship between two classes of minor bodies in our solar system. To provide new insights into D-type asteroids' composition and dynamical evolution and the possible relation with comets, we introduce the mission concept CARINA (Comet Asteroid Relation INvestigation and Analysis). CARINA will visit and collect a sample from the asteroid 2002 AT4 and address key scientific questions related to our understanding of the early solar system evolution, and the origins of water and life on the early Earth. This paper outlines the scientific motivation and the means for the sample return. The spacecraft is equipped with a sampling ring to perform in-situ analysis and to collect, in a "touch and go" manner, samples from the surface and subsurface of the asteroid. A capsule is expected to return the samples to Earth in pristine conditions for detailed and extended analysis. These would represent a rare contribution to our meteorite collection since it would be the first time that material from a D class asteroid would be collected.

1. Introduction

Near-Earth asteroids (NEAs) are one of our closest records of the early Solar System's history and were potential carriers of water and complex organics to the early Earth. In the last twenty years, several sample return space missions were designed and launched toward NEAs [1–3]. Until now, none of them aimed at the exploration of one of the most primitive small bodies - a D-type asteroid. These carbon-rich objects may contain material not yet present in our meteorite collection. D-type asteroids are characterised by a featureless spectrum in the

visible and near-infrared range, a steep red spectral slope, and a very low visual geometric albedo ($p_v \leq 0.05$) [4,5]. Aromatic-type kerogen material is suggested as their main darkening component [6,7]. These insoluble organics may have formed in the early solar nebula under very low temperatures. D-types are mostly localised beyond the outer main asteroid belt and, particularly, in the jovian Trojans, representing around 70% of that population [8–10]. From the main belt inwards their number is significantly lower. They represent around 3% of the known asteroids' population in the near-Earth region [11]. They are

Abbreviations and Acronyms	
AOCS	Attitude and Orbit Control System
D/H	Deuterium-to-Hydrogen
ERC	Earth Return Capsule
GNC	Guidance Navigation and Control
MAC	Mapping Camera
NEA	Near-Earth Asteroid
SAC	Sampling Camera
SIMS	Secondary-Ion Mass Spectrometry
TEM	Transmission Electron Microscopy
TIR	Thermal Infrared
TRL	Technology Readiness Level
VNIR	Visible and Near-Infrared

believed to be among the most primitive class of asteroids, containing primordial organics, volatiles, and perhaps water, either in the form of ice or hydrated minerals. Nevertheless, the exact composition of the D-type asteroids is still uncertain. The study from Earth-based observations is difficult since they are very faint objects. Moreover, the study through the analysis of meteorites is limited since, to date, no confirmed D-type meteoritic sample is known. The closest meteoritic link is the ungrouped carbonaceous chondrite, Tagish Lake [12]. Discovered as it fell to Earth in January 2000 [13], it is a possible fragment from the asteroid (368) Haidea from the main belt [14] or from the NEA 2000 LC16, as recently suggested [15].

D-types' spectra appear to be featureless, although some show a slight curvature at $1.5\,\mu m$ [5]. The presence of water ice can be detected through specific absorption bands, namely around 1.5, 2.0, and $3.0\,\mu m$ [16–18]. Simulations for the trojan asteroid 4709 Ennomos showed that water ice occupying 10% or less of the surface area would be undetectable in the currently available reflection spectra [16]. Additionally, those bands could be weakened due to the amount of organic absorbing matter mixed with the water ice or due to space weathering [19].

In what concerns to their origin, D-types could have formed beyond 15 AU as far as the Kuiper belt before migrating inwards [20] - a migration caused by the dynamic evolution of the giant planets [21]. Thus, D-types could have accreted close to comets, in areas rich in condensed volatiles. Their small fraction in the near-Earth region is mainly a contribution from the 2:1 mean motion resonance with Jupiter and Jupiter family comets [11]. Some of those near-Earth objects, originally classified as primitive asteroids, have been suggested to be extinct comet nuclei. If D-type NEAs could represent extinct comets, they would offer us a unique opportunity to investigate the relationship between two classes of minor bodies in our solar system.

Here we present the mission concept CARINA (Comet Asteroid Relation INvestigation and Analysis) [22]. The goal of CARINA is to return for the first time a sample from a D-type asteroid for an in-depth characterisation in Earth-based laboratories. CARINA aims to:

(i) explore the relationship between dark asteroids and comets;
(ii) investigate the role of dark asteroids in the origin of life;
(iii) improve our understanding of early Solar System evolution.

This paper is organised as follows. In Section 2 we briefly address the topics that form the CARINA science case. Scientific objectives and requirements, the target (the Amor asteroid 2002 AT4), and the importance and need of sample return are described in Section 3. In Section 4 we present the mission analysis, which includes trajectory, landing and Earth re-entry. In Section 5 we describe CARINA's spacecraft and respective subsystems. In Section 6 we present important aspects of sample curation. Lastly, we draw some conclusions and remarks in Section 7.

2. CARINA science case

2.1. Asteroids and comets: exploring the continuum

Traditionally, asteroids and comets are addressed as two distinct groups of small planetary bodies. The distinction is mainly based on their orbital cycle and composition. However, some bodies seem to cross these boundaries, such as asteroids in "comet-like" orbits [23] and active asteroids ejecting dust [24,25]. This gave rise to a so-called asteroid–comet continuum [26–28], an approach that best reflects the interrelationship between these two classes of small bodies.

The existence of extinct comets in the near-Earth region has been discussed since the 1960s [29,30]. The increasing number and developments in ground-based observations of the near-Earth population indicate that contributions from comets are perhaps more common than previously thought. A significant part of them may be disguised as dark asteroids (C, D, P, T taxonomic types) [31]. While some of the objects seems to be inert, others do not. The Amor asteroid (3552) Don Quixote, classified as a D-type asteroid and a possible dormant comet, shows intermittent cometary activity [32]. More recently the OSIRIS-REx mission revealed that (101955) Bennu is an active asteroid [33]. Among the possible mechanisms responsible for Bennu's ejection of particles are meteoroid impacts and thermal fracturing [34,35].

The possible extinct comets in the near-Earth region can be recognised using the jovian Tisserand parameter, T_j [24]. In short, objects with $T_j < 3$ are essentially dynamically coupled with Jupiter and are considered to have 'comet-like' orbits, while objects with $T_j > 3$ are commonly considered to have 'asteroid-like' orbits. Nevertheless, non-gravitational forces, such as cometary outgassing, can affect this parameter [36], as well as a possible interaction of near-Earth objects with the inner planets. Therefore, $T_j < 3$ is not a rigid but rather a flexible limit. DeMeo et al. estimated that around 8% of asteroid-like objects in the near-Earth population are strong comet candidates [37].

The method of a comet becoming extinct is not well understood. One theory suggests a non-volatile crust can form on the surface, which can repress subsurface volatiles from subliming, rendering the comet inactive. These non-volatile grains are left behind or launched from the surface of the comet as volatile gas and dust which sublimes before falling back to the surface [38], as illustrated in Fig. 1.

In order to recognise the relationship between comets and dark asteroids, such as D-types, one must have knowledge of the properties of both entities. We learned about comets from the Stardust [39] and Rosetta [40,41] space missions. In the future, we will have the contribution of the Comet Interceptor mission [42]. However, detailed information from the D-types (the spectral class that best matches comet nuclei) is still missing, leaving us without enough material for comparison. CARINA would visit a D-type asteroid in the near-Earth region with the purpose of investigating how likely D-types are extinct comets. It would allow us to estimate how many of the current objects can still be considered to be good extinct comet candidates.

2.2. Astrobiological relevance of primitive asteroids

Our understanding of the origin and evolution of life on Earth relies on the study of the sources of water, energy, and prebiotic organic molecules. Primitive asteroids were potential carriers of a bunch of prebiotic organic molecules to the early Earth. An extended variety of indigenous organic compounds were found in carbonaceous chondrites, which include hydrocarbons, amino acids, sugars, and nucleobases [43]. Amphiphiles, molecules that can spontaneously self-assemble into membranous structures, were also detected [44]. Chemical analysis of meteorites, together with petrological studies, have been showing that the content and the variety of organics is likely to be correlated with the degree of aqueous alteration of the meteorite parent body [45].
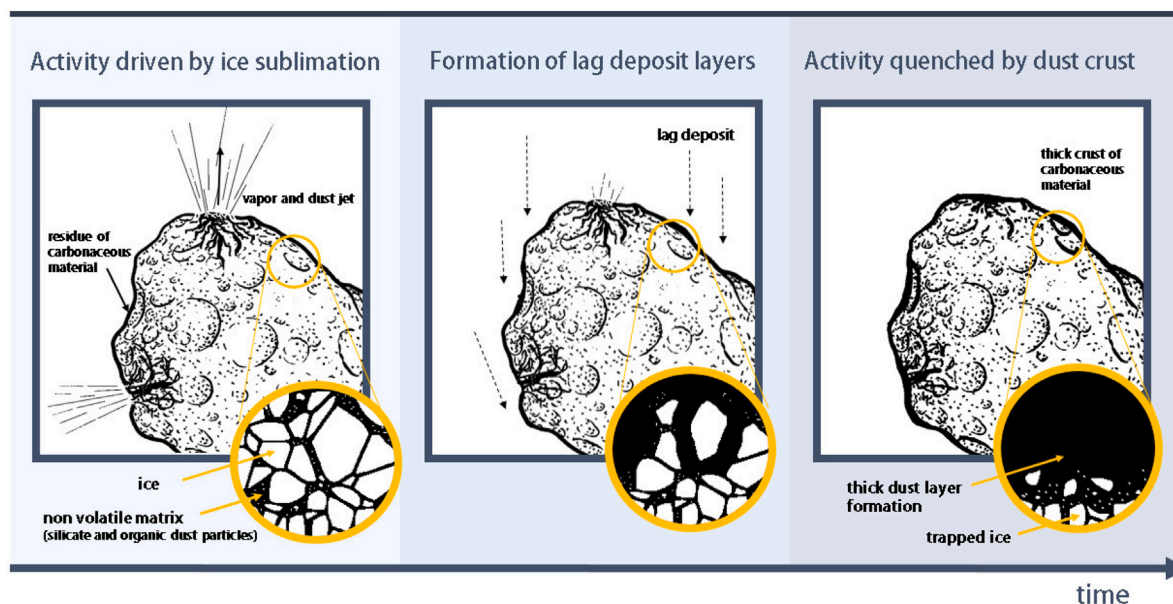
Fig. 1. Comet quenching scheme. During perihelion passages, water and other icy volatiles sublimate from the nucleus's surface. Dust is ejected through ruptures from gas pressure and thermal stress fractures (left). A surface layer starts forming from the lag deposit of non-volatile grains (middle). A ticker crust grows insulating the remnant underlying ices from sublimation (right).

The homochirality of life is still a major puzzle in the research of the origin and evolution of life. Living organisms preferentially use L-aminoacids, the building blocks of proteins, and D-sugars, the building blocks of the nucleic acids DNA and RNA. The reasons behind this biomolecular asymmetry remain unclear. However, enantiomeric enhancements were observed in some meteoritic organic compounds [46], demonstrating that molecular asymmetry is not necessarily influenced by terrestrial conditions.

With regards to Earth's water, its origin is still under intense debate. Several scenarios have been considered [47], including the exogenic delivery from comets. However, values for the deuterium to hydrogen (D/H) isotopic ratio from cometary reservoirs are usually higher than Earth's oceans, as observed for the comet 67P/Churyumov-Gerasimenko which is larger by roughly a factor of three [48]. Thus comets are perhaps only a part of the delivery [49] and attention turned to primitive asteroids. The D/H isotopic ratio and δD of bulk carbonaceous chondrites are known to be close to the Earth's water [50,51]. CARINA aims to investigate the possible role of D-types in the delivery of organics and water to Earth, helping to validate or dismiss some of the current hypotheses.

2.3. The solar system evolution

The origin and dynamical evolution of D-type asteroids are still largely unknown [52]. Recent dynamical models based on the Nice model [53] suggest that D-types were formed in the outer Solar System, i.e., beyond Neptune's orbit, and then some of them were "transported" to their current locations due to the giant planets' migration [10]. This was first suggested and simulated using the original Nice model framework by Levision et al. [21]. However, there are two main issues with their results. First, the number observed of P and D-type asteroids in the main belt is smaller than what is predicted by the simulation results. Second, their simulation results show that D-types and other captured planetesimals do not reach the inner main belt, which disagrees with recent reports of D-types beyond that belt [10,54,55]. The latter issue was surpassed by the results obtained by Vokrouhlický et al. [56] which presented a model that retrieved for the first time, a D-type asteroid population in the main belt. However, the number of P-/D-types obtained is lower by a factor of 3 than the observed population.

Their results led the authors to predict that near-Earth D-types on low delta-V orbits are relics from the original population, beyond Neptune [55,57]. Questions regarding the D-types' composition, variation of the composition with the heliocentric distance, and their relationship with existing meteorites remain unanswered. For this reason, more observations are required at a large wavelength range [57] as well as a pristine sample to be analysed on Earth.

2.4. Tagish Lake meteorite and the lack of a sample

Within the meteorites in our available collection on Earth, Tagish Lake was the first to be reported as a possible representative of a D-type asteroid [12] and it is still the best match so far. Other candidates are the CM2 Meteorite Hills (MET) 00432, the CM-anomalous Wisconsin Range (WIS) 91600, and more recently the C2-ungrouped Tarda meteorite [58,59]. Tagish Lake is a petrologic type 2 carbonaceous chondrite. Considering its distinct mineralogy, isotopic and whole-rock chemical composition, it fits somewhere between the CI and CM groups, remaining for now ungrouped. The meteorite is a breccia. Its large matrix fraction supports small olivine-rich aggregates and calcium, magnesium, iron and manganese carbonates. Subtle and dispersed chondrules were also found. Its trace elemental analysis is reported elsewhere [60]. Although it is a carbon-rich meteorite, the apparently low amino-acid content found in Tagish Lake put into question whether D-type asteroids are rich in biologically-relevant organic compounds. One of its unusual physical features is its extremely low bulk density, around $1.7\,\mathrm{g/cm^3}$, which is related to its high porosity [61]. The value is lower than the typical for the CI meteoritic group where the bulk density is around $2.3\,\mathrm{g/cm^3}$. This characteristic could be associated to an origin far from the Sun [61,62].

It was proposed that Tagish Lake represents a new kind of type 2 carbonaceous chondrite [61,63]. A new sample would help to understand if the Tagish Lake is an anomalous member, as a less altered CI chondrite, or a first representative of a new group. Thus, similarities between Tagish Lake meteorite and others (e.g., Tarda) with D-types are worth exploring.

Table 1
Scientific goals and respective scientific objectives.

Scientific goals	Scientific objectives
Investigate the asteroid-comet relationship	- Characterise a D-type asteroid - Compare the physico-chemical properties of D-types with comet nuclei - Evaluate whether D-types could represent extinct comet nuclei - Investigate the mechanism pathway of comet quenching
Investigate the origin of life	- Explore the amount and diversity of organic material - Investigate the enantiomeric distribution of the organic material - Investigate the presence of water and its isotopic variation - Link D-type asteroids to potential meteorite analogues
Improve our understanding of the early Solar System evolution	- Estimate the timescales of accretion and planetesimal formation - Characterise mixing of elements in the protoplanetary disk - Characterise the conditions of the early outer solar nebula - Check validity of formation models

3. Mission overview

3.1. Science objectives

The scientific objectives address by CARINA are divided into three major categories, which we will describe below, and are summarised in Table 1.

Exploration of the asteroid–comet continuum

How likely is it that near-Earth D-type asteroids represent extinct comet nuclei? If D-type NEAs represent extinct comets, they would offer us a unique opportunity to investigate the relationship between two classes of minor bodies in our solar system. CARINA aims to perform detailed characterisation of a D-type asteroid. It will determine the volatile content, the porosity, and the effect of space weathering on the surface. Compositional and physical maps can be compared to data from ESA's Rosetta [41] and NASA's Lucy [64] missions. In particular, CARINA aims at searching for evidence of comet quenching. This requires a sample collection from the subsurface, where there might be hydrated minerals and cometary-like material still present. Laboratory measurements of the returned material, will be important, since the exact same experimental procedures and conditions can be replicated from analysis on Stardust, Hayabusa2, and OSIRIS-REx samples. These will likely include electron microprobe analysis (EMPA), gas pycnometry, microcomputed tomography, scanning electron microscopy (SEM), secondary ion mass spectrometry (SIMS), Raman spectroscopy, transmission electron microscopy (TEM) and X-ray absorption spectroscopy (XAS) analysis.

Understand the origin of life on Earth

What role did D-type asteroids play on Earth's evolution and the emergence of life? CARINA would explore the presence of water and the presence, abundance, and diversity of soluble organic compounds on 2002 AT4. The goal is to learn whether these objects were involved in the extraterrestrial delivery of organics and water and to what extent. On Earth, techniques such as gas chromatography mass spectrometry (GC–MS), nuclear magnetic resonance (NMR), Raman Spectroscopy and circular dichroism will be fundamental for chemical analysis and isotopic signatures.

D-types origin and evolution in the solar system

What were the conditions behind our solar system evolution and planet formation? Where did D-types form and how did they reach the near-Earth region? The analysis of the pristine material collected by CARINA could offer relevant constraints on the solar system formation and the evolution of primitive asteroids. Calcium–aluminium inclusions and chondrules might be present in the collected samples and are meticulous records of the processes that operated inside the solar protoplanetary disk. Dating sample minerals, such as carbonate salts that suffer aqueous alteration, provide constraints on the accretion ages of the parent body. Some of the analysis to be performed on Earth includes laser ablation inductively coupled plasma mass spectrometry (LA-ICP-MS), SIMS, energy-dispersive X-ray spectroscopy (EDS), and superconducting quantum interference device (SQUID) magnetometry.

3.2. The importance of a sample return

Though we have limited samples of carbonaceous meteorites, their value is compromised by the lack of geologic context. Both meteorite falls and finds experience uncontrolled contamination as soon as they reach the ground, invariably affecting the analysis and quantification of their chemical composition, meaning that they are no longer pristine samples. A major advantage of any sample return mission is that the samples experience little to no terrestrial exposure, minimising contamination. The sampling site can also be chosen and analysed in-situ before sample collection, providing the necessary geological context. In the end, the sample can be selected as a representative of the body itself. As discussed previously the scientific objectives of CARINA's mission require analysis of pristine material with known geological context. To get the necessary answers, high-resolution analytical techniques are essential. Some of them are complex, heavy, or highly specialised in terms of instrumentation and thus only available on Earth (e.g. TEM). It is also important to keep in mind that sample return missions are timeless. The returned material can be stored and kept for future scientific questions and be analysed by novel techniques yet to be developed or improved.

3.3. Target 2002 AT4

CARINA's spacecraft would visit the Amor asteroid 2002 AT4 that was observed under the framework of the Small Main Belt Spectroscopy Survey in the visible and near-infrared spectroscopy window (Fig. 2). It was classified as a D-type asteroid in the Bus (1999) taxonomic system by Binzel et al. [65], and was also pointed as one of the potential candidates of extinct comets in the near-Earth region. Therefore, considering aspects such as low-ΔV and asteroid size, it is a suitable mission target for CARINA. The major parameters (observed and estimated) of 2002 AT4 are listed in Table 2.

The rotational period of 2002 AT4 has been assumed as ~6 hours in the Don Quijote mission statement of work, based on the average of rotational period values for asteroids with a diameter of ~500 m [67]. However, no extensive observations have been performed in order to estimate its spin state. The minimum rotational period of the asteroid can be considered to be 2.2 h - a threshold called "spin barrier" derived by the rotational statistics of asteroids [68].

3.3.1. Sub-solar surface temperature estimation

In what follows, we will estimate the maximum sub-solar surface temperature of the 2002 AT4 asteroid. Then, in Section 3.3.2, we will use this value to simulate the sub-surface temperature at different depths to gain insight into the minimum sampling depth needed to collect possible volatiles, namely water.
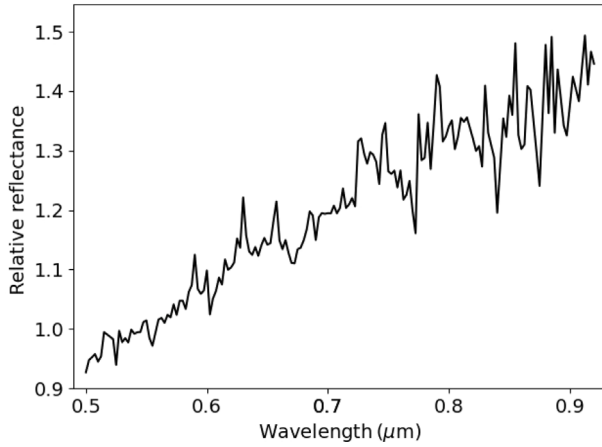
Fig. 2. Relative reflectance spectrum of the D-type asteroid 2002 AT4 [65].

Table 2
CARINA's target characteristics. a: semi-major axis; H_{mag}: absolute magnitude; ΔV: velocity budget; T: rotational period; T_J: Jupiter Tisserand parameter. JPL: Jet Propulsion Laboratory Small-Body Database.

Parameter	Value	References
Designation	2002 AT4	[65]
Taxonomy	D	[65]
Orbit	Amor	JPL
Period (years)	2.55	JPL
a (AU)	1.867	JPL
Eccentricity	0.447	JPL
Inclination (degrees)	1.499	JPL
Perihelion distance (AU)	1.034	JPL
Aphelion distance (AU)	2.701	JPL
H_{mag}	20.9 – 21.4	[36,65]
ΔV (km/s)	5.6	[57]
T (h)	6	[66]
Diameter (m)	349	[57]
T_J	3.95	[65]
Density (g/cm^3)	1.3 – 2.3	[61]

The surface temperature of an asteroid depends on its heliocentric distance, its surface material and texture, its spin state, and also its shape [66]. The maximum sub-solar temperature T_{SS}^{max} of an airless celestial body is calculated by the formula [69]:

$$T_{SS}^{max} = \sqrt[4]{\frac{(1 - A)S_0}{r^2 \epsilon \sigma}}, \tag{1}$$

where A is bond albedo, S_0 is the solar constant, r is the heliocentric distance in AU, ϵ is the emissivity, and σ is the Stefan–Boltzmann's constant. The bond albedo A is related with the visual geometric albedo p_V through the following approximation [69]:

$$A \approx q\, p_V, \tag{2}$$

where q is the phase integral and is given by

$$q = 0.290 + 0.684\, G, \tag{3}$$

where G is the slope parameter. The latter is considered to be 0.15 for most asteroids [69,70], while the value for the emissivity ϵ is assumed to be 0.9. D-types are observed to have mainly a p_V of 0.04 [71]. Considering these values, the albedo of a D-type asteroid can be estimated as $A \sim 0.0157$. Therefore, the maximum sub-solar surface temperature of 2002 AT4 can be calculated by using Eq. (1), which gives $T_{SS}^{max} = 295.26$ K at the aphelion and $T_{SS}^{max} = 396.84$ K at the perihelion.

3.3.2. Subsurface temperature estimation
Heat from the surface of the asteroid is transferred to its inner layers. The depth at which the diurnal thermal wave reduces its amplitude

to $1/e$ of its surface value is called the skin depth, l_s. The latter is calculated as [72,73]:

$$l_s = \sqrt{\frac{k_s}{\rho_s\, c_s\, \omega}}, \tag{4}$$

where k_s is the thermal conductivity coefficient, ρ_s is the density, c_s the specific heat capacity and ω the rotational angular velocity. The typical skin depth values for asteroids are $10^{-3} - 10^{-2}$ m [74]. Here we assumed that D-type asteroids have approximately the same density as C-type asteroids. Observations from NEAR-Shoemaker spacecraft have shown that the main belt primitive C-type asteroid, 253 Mathilde, with ~50 km diameter has a bulk density of 1.3 ± 0.2 g/cm^3 [75]. Moreover, the thermal conductivity and specific heat capacities for CM chondrites are $k_c = 0.5$ W/m/K [76] and $c_s = 500$ J/kg/K at 200 K [77] respectively, which we assumed as a good approximation considering that D-types surface composition is likely similar to carbonaceous chondrites. Using the values above, the estimated skin depth of the asteroid 2002 AT4 is $l_s \sim 0.03$ m for a rotational period of 2.2 h and $l_s \sim 0.05$ m for a period of 6 hours.

A rough estimation of the subsurface asteroid's temperature was performed using Energy 2D [78], a free software for solving heat diffusion equations. The simulation was executed on a 2D box ($2\,m \times 2\,m$), which is defined as homogeneous regolith material without porosity and with the same value of density used previously to estimate the skin depth and with the same thermal properties. The top boundary was considered as the asteroid's surface and the bottom boundary was considered as the subsurface at 2 m depth. The left and right borders do not reflect or absorb the heat. The initial (background) temperature of the material was considered to be 200 K as a mean temperature of a shadowed body at the vicinity of Earth–Mars [79,80]. The top boundary was considered to have a stable temperature, namely, the maximum sub-solar surface temperature of 2002 AT4 at perihelion, $T_{SS} = 396.84$ K, and defined as reflective to enable a deeper transfer of heat through the regolith. Moreover, the gravitational acceleration was assumed to be of the order of 1×10^{-7} m/s^2. During the execution of the simulation, heat flows from the surface to the deeper layers, changing their temperature as a function of time. The results are presented in Fig. 3, showing the temperature growth with depth as function of the solar exposure time of the asteroid's surface. The real exposure time of 2002 AT4 is equal to half of asteroid's rotational period, which is unknown. In order to find possible volatiles in an asteroid, the sampling location must have a property temperature. The temperature for the chemisorbed water's desorption is at ~225 K. Therefore, this temperature can be found at a depth of ~0.12 m for a rotational period of 2.2 h and ~0.18 m for a rotational period of 6 h. Based on this estimation, 15 to 20 cm of depth seems to be more than enough for our subsurface sampling so that, if chemisorbed water is present, we can collect it.

3.4. Scientific payload

The CARINA spacecraft (described in Section 5) will carry seven scientific instruments on board: mapping and sampling cameras, a visible and near-infrared spectrometer, a thermal infrared spectrometer, a mass spectrometer, a subsurface radar, and a magnetometer. These instruments were chosen in order to:

1. Enable safe operations and facilitate sample site selection;
2. Place the samples in their global and local context;
3. Collect the material and perform in-situ analysis;
4. Provide complementary science.

Their objectives and respective requirements are summarised in Table 3. We will next describe them in more detail.

Table 3
Overview of the scientific payload.

Instrument	Goal[a]	Objective	Measurement requirement
Mapping Camera	1, 2	Global mapping; Shape model; Geological context; Preliminary landing site selection	50 cm resolution
Sampling Camera	1, 2, 4	Local mapping; Surface topography and morphology; Sampling site selection	10 cm resolution
Visible/Near-Infrared Spectrometer	1, 2, 4	Surface composition and mineralogy	$0.4 - 4.3\,\mu m$ bandwidth, spectral resolution of 30 nm
Thermal Infrared Spectrometer	1, 2, 4	Thermal inertia; Thermophysical modelling (size and shape), Bond albedo, Sampling site temperature	$5 - 20\,\mu m$ bandwidth, spectral resolution of $0.5\,\mu m$
Subsurface Penetrating Radar	1, 2, 4	Near subsurface characterisation, Ranging topography	$3 - 4\,m$ penetration depth minimum, $1 \times 1\,m$ resolution
Mass Spectrometer	3, 4	In situ compositional characterisation of samples; Identification of volatiles and organics	$5 - 60\,m/z$ range, 5% detection limit
Magnetometer	4	Magnetic field measurements	$< 10\,pT$
Bristle Sampling Tool	3	Surface sample collection	10 g
Harpoon Sampling Tool	3	Subsurface sample collection	10 g

[a]Numbers 1 to 4 refer to the goals listed in the beginning of Section 3.4.
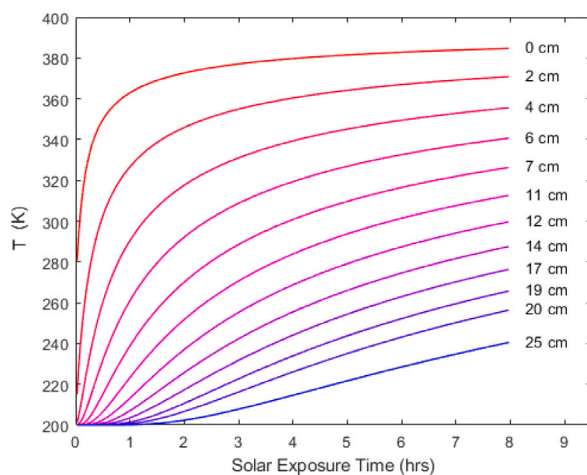
Fig. 3. Simulated subsurface temperature of 2002 AT4, in the perihelion, as a function of the solar exposure time for different depth values.

3.4.1. Mapping camera

The main objective of the mapping camera (MAC) is to obtain a shape model of the asteroid. The shape can be determined if the entire body is included in one MAC image while the spacecraft is in a distant orbit (about 5 km), which also allows its global characterisation. From the surface map, a preliminary sampling site will be selected. MAC images will also be used for determining the rotation rate of the asteroid. Taking advantage of the wide field of view, the camera will search for any potential 'moons' around the asteroid. Finally, the MAC may also be used to support navigation purposes, in particular during the approach phase. The MAC has heritage from the OSIRIS Wide Angle Camera [81] that flew on board the Rosetta spacecraft and from the Wide Angle Camera proposed for ESA's MarcoPolo-R mission [82] thus has a technology readiness level (TRL) of 4.

3.4.2. Sampling camera

The purpose of the sampling camera (SAC) is to image narrow portions of the asteroid's surface with high resolution. The SAC is thus capable of imaging the surface with a 10 cm resolution, which provides the minimum resolution needed to identify the best landing and sampling sites. These images will be also used for the characterisation of the surface topography and morphological features and to analyse

regolith fragmentation and accretion. Thus, SAC will help to estimate the bulk composition of the body. The SAC imaging will also bring complementary details of the shape model obtained from MAC and close characterisation of any moons that might be discovered. Finally, the SAC may also be used for spacecraft navigation during sampling. It would be built on heritage from the Close-Up camera proposed for ESA's MarcoPolo-R mission [82,83] and thus has a TRL of 4.

3.4.3. Visible and near-infrared spectrometer

The visible and near-infrared (VNIR) spectroscopy will characterise the surface composition of the asteroid. It will explore the mineralogical and chemical composition that can be linked with the surface morphology data and, therefore, help in sampling site selection. Spectra in a broad wavelength range are needed to identify the mineralogical diversity on the asteroid surface and also expected organic compounds. The spectrometers will be used to image in the visible and near-IR wavelength range from $0.4\,to\,4.3\,\mu m$ (i.e. $2325 - 25000\,cm^{-1}$) and a spectral resolution of less than 30 nm. The spectrometer heritage comes from the NIRS3 on Hayabusa2 [84] and OMEGA that flew on board Mars Express [85] and therefore has a TRL of 9.

3.4.4. Thermal infrared spectrometer

The thermal infrared spectrometer (TIR) will provide qualitative and quantitative information on surface composition and mineralogy (e.g. organics and silicates). This compositional information complements data from VNIR spectroscopy providing a global context for the returned samples. TIR will also study the asteroid surface thermal inertia and hence the magnitude of Yarkovsky and YORP thermal effects. Moreover, information about surface roughness, regolith particle size, and regolith thickness will be useful for a better sample site selection. The TIR instrument has a TRL of 9 and heritage from the Compact Modular Sounder that flew onboard the TechDemoSat −1 satellite, and from the thermal mappers proposed for CASTAway and Castalia missions [86,87].

3.4.5. Mass spectrometer

The mass spectrometer is responsible for the detection, quantification, and isotopic compositional study of volatiles. Namely, the presence of major species (e.g. water, CO, CO_2 and NH_3) and trace organic species (e.g. CH_3OH, CH_4O) will be explored. In case collected samples are not returned intact to Earth, the mass spectrometry data obtained in situ ensures that important scientific return is still provided (e.g water D/H ratio). Moreover, this data will help to detect possible contaminations or physicochemical alterations during the return trip

or during the capsule opening procedures. The instrument is inspired by the gas chromatograph-isotope ratio-mass spectrometer Ptolemy carried by Philae [88,89] and has a TRL 9.

3.4.6. Shallow surface penetrating radar

CARINA's spacecraft will carry a radar inspired by the monostatic high-frequency radar design for the Asteroid Impact Mission [90] and has TRL of 4. The radar will investigate the shallow subsurface of the asteroid down to a few tens of metres depth with metric resolution. This resolution is suitable for the study of the regolith structure, its size distribution, depth, stratigraphy, and heterogeneities. It would provide better constraints on the process of regolith formation, evolution, and thermal state. Furthermore, by knowing the characteristics of the regolith around the sampling site, we obtain important sample geological context and vertical layering information. Thus, radar data complements our spectroscopy measurements.

3.4.7. Magnetometer

The magnetometer onboard CARINA's spacecraft will measure any intrinsic magnetic field of the asteroid or any residual remanent magnetisation. It will mainly provide complementary information to fulfil the scientific objectives (e.g. constraints on the thermal and aqueous evolution of the target, and investigation of effects such as the magnetochiral dichroism). There is limited knowledge from previous magnetic field observations, therefore it will be interesting to compare the magnetic properties of CARINA's target with the ones from a comet (Rosetta), from a C-type asteroid (Hayabusa2) and other carbonaceous chondrites from our meteorite collection. The magnetometer has a TRL 9 since it will be similar to MASMAG on the MASCOT rover from Hayabusa2 [91].

3.5. Sampling mechanisms

The bristle sampler is the basic mechanism to collect surface samples of the regolith. It has the capacity to collect a total of $43\,cm^3$, which corresponds to a maximum of about 100 g. The sampler uses two rotating bristles ("brushes") that lift up the particles of soil. These particles pass through a central opening between the bristles and end up stored in a sample container. It was proposed for Phobos sample return and has a TRL of 3-4 [92]. Two bristle samplers are considered for reliability.

The Harpoon Sampler [93] collects subsurface samples. Tests with different materials have shown a penetration depth of up to $24\,cm$. The harpoon has two shells, the outer shell will stay in the asteroid and the inner one will be pulled back out, along with the sampled subsurface regolith. Two harpoons are considered for reliability, each with the possibility of collecting $15\,g$. The technology has a TRL of 4.

4. Mission analysis

4.1. Interplanetary trajectory

The present mission to the NEA 2002 AT4 would be launched from the European Launchpad in Kourou, the Guiana Space Centre, onboard the Ariane 62 launcher [94]. The Ariane 62 has been chosen since it can provide the necessary mass at launch to perform the sample return mission. Direct injection is used to deliver the spacecraft into the heliocentric transfer orbit.

An initial trade-off analysis between chemical and electric propulsion has been performed. For the chemical propulsion, impulsive maneuvers were first considered, and porkchop plots have been generated assuming Lambert transfers between the orbits for different departure dates and times of flight. Hence, a global optimiser was run to find the optimal combination of departure date and transfer time to minimise the total ΔV. Considering preliminary values of the spacecraft's initial mass and specific impulse of $2000\,kg$ and $320\,s$, respectively, an

Table 4
Potential mission scenarios within the 2030–2035 launch timeframe.

Launch date	29/06/2030	12/08/2033	31/08/2035
Mass at launch (kg)	1825	2012	2039
Duration (years)	6.9	6.5	6.7
Stay time (months)	7	22	7

Table 5
Interplanetary transfer (IT) phases and respective dates for the first launch window.

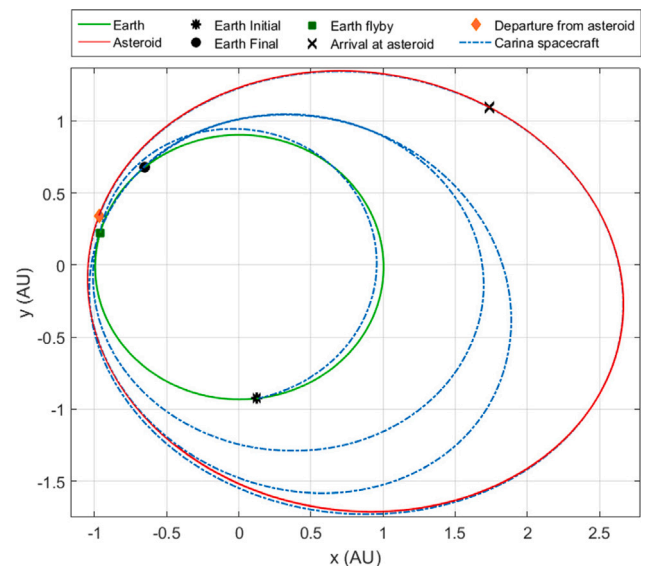| IT phases	Date
Earth departure	29/06/2030
Earth swing-by	07/03/2031
Arrival at 2002 AT4	26/09/2034
Departure from 2002 AT4	24/04/2035
Earth re-entry	31/01/2037

Fig. 4. CARINA's interplanetary trajectory.

excessive amount of fuel consumption was obtained (about $1740\,kg$). Therefore, it has been stated that mission objectives could be better satisfied by employing electric propulsion, in particular by using two T6 ion engines. For the transfer towards the asteroid 2002 AT4, an Earth flyby has been considered to decrease the total fuel consumption. Therefore, some simulations have been performed by means of the software Pagmo [95] to identify several possibilities for the departure of the CARINA spacecraft. The results are shown in Table 4, in which three different launch dates within 2030–2035 are proposed.

Among them, the first launch window (29th of June 2030) has been chosen for the analysis presented in this paper. Once the ongoing trajectory was obtained, the returning path (to the Earth) was computed and optimised using the software SNOPT [96]. The entire trajectory is shown in Fig. 4 with the dates corresponding to the main phases of the interplanetary transfer illustrated in Table 5. The estimated propellant consumption of the ongoing and returning phases are respectively $486\,kg$ and $202\,kg$.

4.2. Proximity operations

For the proximity operations at the asteroid, the landing and ascent trajectories were computed using successive convexification minimising propellant consumption as described in [97] with the SCOPT optimiser [98]. At this time of the feasibility study of the CARINA mission, the exact rotational period and shape of the asteroid have not been

determined. The assumption of a spherical shape was carried out to retrieve the optimal landing and ascent trajectories using a successive convexification algorithm. This would represent initial guess trajectories to estimate the fuel consumption, and could be thought of as reference trajectories to be tracked. Indeed, an advanced autonomous guidance employing model predictive control, as based on convex optimisation, and/or other robust control strategies, such as a sliding mode control, could be used to follow the computed reference trajectories, while accounting for the perturbations induced by the real irregular shape of the asteroid, and still obtain some theoretical stability guarantees. The approach might provide a slightly bigger fuel consumption than that computed with the proposed spherical shape of the asteroid. However, since the real shape of the asteroid is not currently known, the proposed assumptions are considered suitable enough for a preliminary study. Considering the asteroid's shape as a sphere, a central gravitational field is assumed with an asteroid rotating period of 4 h. One should note that this represents a mean value with respect to the probable two values given in Section 3.3. The spacecraft descents, from an initial orbit of 1 km in radius, towards a landing site located at 20° of latitude and 40° of longitude, with a 60° glide-slope and final tilting constraints. It is then assumed that the spacecraft ascends towards the initial orbit once the surface operations are completed. Only one reaction control system thruster with a maximum and minimum thrust setting of 20 N and 5 N, respectively, is assumed, resulting in a low propellant consumption and a thrust profile using the least force setting. The trajectory results can be seen in Table 6 and Fig. 5 for the landing manoeuvre.

In particular, during the landing trajectory, the spacecraft first turns the solar panels 25° upwards, providing clearance from possible boulders or slopes. It then proceeds by performing a propulsive landing using its attitude and orbit control (AOCS) thrusters to decelerate from orbit. Around 8 m before touchdown, the thrusters are turned off, and a free-fall is performed in order to avoid ground contamination [99]. Once the accelerometers detect a ground impact at approximately 6 cm/s, the upper thrusters are turned on in order to avoid a re-bounce and attach the spacecraft to the ground, providing active damping in combination with four landing legs (heritage from Phobos sample return [100], and a TRL ≥ 4). The sample retrieval procedure is performed as explained in Section 3.5. Once the sample is retrieved, the lower thrusters are turned on and the spacecraft returns to orbit.

The low propellant mass consumption resulting from a closed loop optimum based guidance and control algorithm would allow for multiple landing attempts and hovering trajectories, which are important to scan the surface of the asteroid for possible boulders and to find a safe landing point.

A closed-loop GNC module would be required to perform accurate proximity maneuvers. In particular, the proposed method could be used to quickly obtain the reference optimal trajectories to be tracked by a robust control (eventually considering additional perturbations). The actual state of the spacecraft to be employed for the control would be provided by a filter which processes the observables coming from the sensors onboard the spacecraft.

4.3. Earth re-entry

A preliminary entry trajectory analysis was performed using semi-empirical analytical equations for a ballistic re-entry given an assumed ballistic coefficient and entry conditions [101]. The resulting maximum heat fluxes and heat load was used to size the Earth return capsule nose radius and thermal protection system to ensure adequate aerothermal loads for the sample. The resulting re-entry mission phases are illustrated in Fig. 6.

The recovery phase starts around 10 days prior to atmospheric entry (T_0). The spacecraft performs a correction maneuver targeting the Earth atmosphere. Around 36 h prior to entry, the spacecraft performs an additional correction to further enhance the entry accuracy. Then spins

Table 6
Proximity operations results.

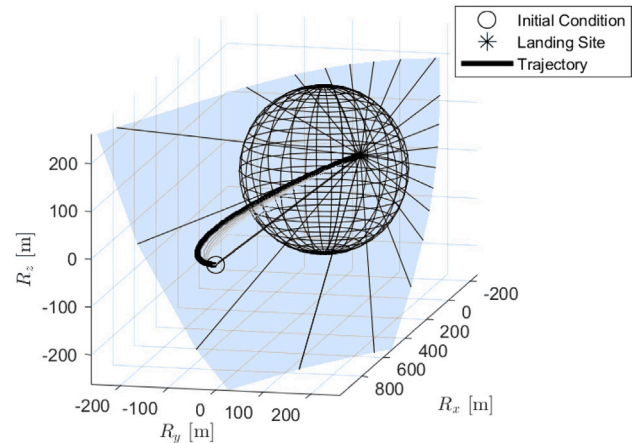| Phase	Descent and landing	Ascent
Duration [s]	981.2	960.65
Propellant [kg]	2.196	2.129
ΔV [m/s]	3.705	3.597

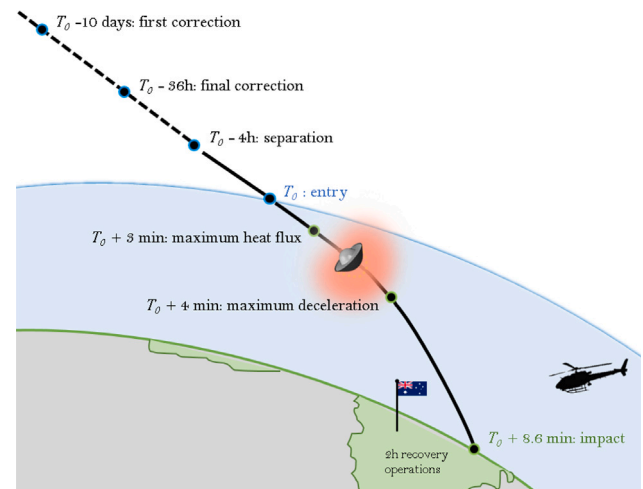**Fig. 5.** CARINA's descent and landing manoeuvre.

Fig. 6. Earth re-entry phases.

up and deploys the Earth return capsule at $T_0 - 4$ hours towards its final destination and continues its deflected hyperbolic trajectory surpassing the Earth. The crushable capsule then enters the Earth's atmosphere with an approximate re-entry velocity of 12.15 km/s and a flight path angle of −15°. Shortly afterwards, the maximum heat flux is experienced followed by a maximum deceleration. The proposed capsule, described in Section 5.5, then performs a direct impact on the ground without the use of any parachute. The feasible preliminary design results for the trajectory and impact are the following:

a Maximum deceleration of $a_{\max} = 84$ g.
b Heat flux rate of $\dot{q}_{max} = 10.3$ MW/m^2.
c Heat flux per unit area of $Q/A = 261$ MJ/m^2.
d Impact deceleration of $a_i = 678$.

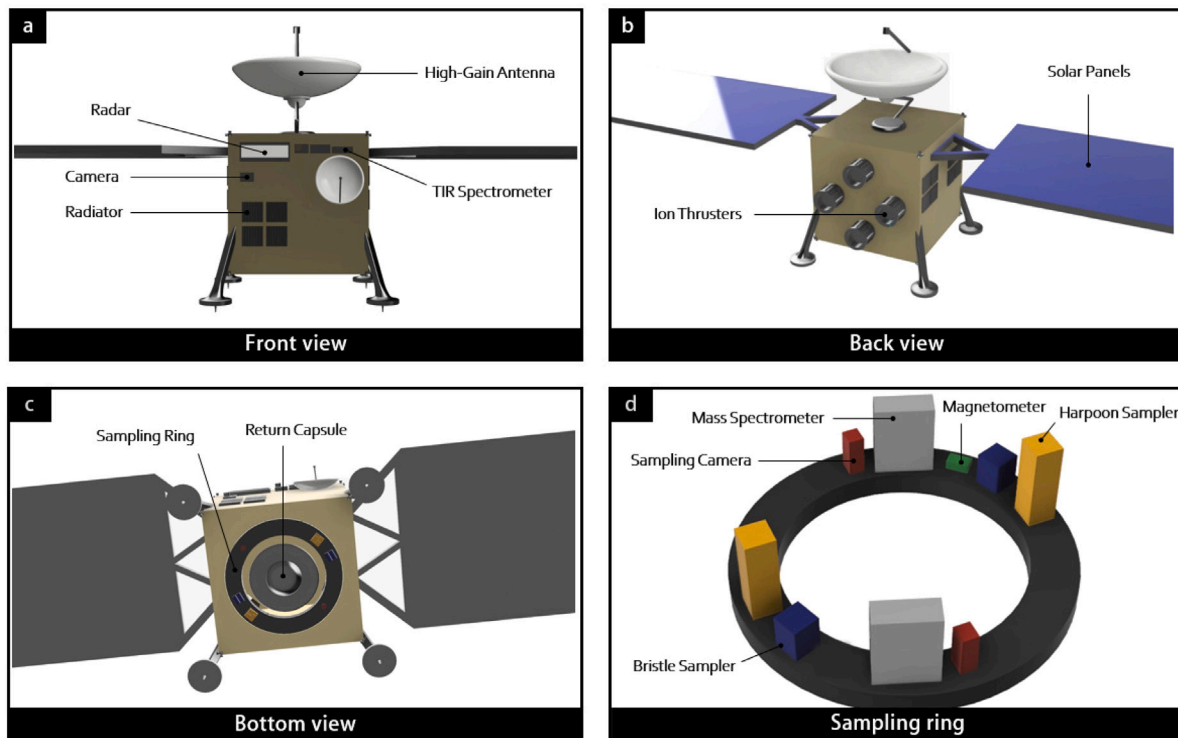For landing sites, terrain landings in Australia, Ohio (USA), and Kazakhstan were considered.

Fig. 7. Carina spacecraft (S/C) in deployed configuration. It will be powered by a solar array and propelled by ion thrusters. (a) S/C front view. (b) S/C back view. (c) S/C bottom view with the return capsule and sampling ring. (d) Artistic impression of the sampling ring with the allocated scientific instruments and sampling tools. The instruments that are mounted in the bottom plane of the ring are the samplers and the cameras, as shown in (c).

5. Spacecraft subsystems

The CARINA's spacecraft, illustrated in Fig. 7, would be powered by two $5\,m \times 2\,m$ foldable solar panels, and propelled by 2×2 ion thrusters. It accommodates a sampling ring that is capable of rotating. The sampling ring would accommodate the samplers (bristle and harpoon) and some scientific instruments, namely, the sampling camera, the mass spectrometer, and the magnetometer. The sampling ring rotation allows moving the devices to a certain degree, which helps to avoid undesirable sampling locations (such as undesirable boulders) and to select specific sites that might be of interest. Therefore, this mechanism gives some degree of freedom and increases the likelihood of the retrieval of sufficient and adequate samples.

The main subsystems of CARINA are explored below.

5.1. Attitude and orbit control

The most important pointing requirement is the pointing of the X-Band Antenna. For this, we defined the following requirements:

1. 700 arcsec pointing accuracy
2. 70 arcsec knowledge accuracy
3. 0.1 mN·m disturbance (worst case)

In order to accomplish these tasks, the AOCS is made up of attitude and position determination sensors, such as star trackers, gyro and laser range finder, and actuators, such as reaction wheels and hydrazine thrusters. Table 7 shows the features of the chosen devices together with the associated TRL.

5.2. Propulsion

The propulsion system consists of the main engines for the interplanetary transfer orbits and the attitude and control thrusters, already proposed in the previous section. Since initial computations showed excessive propellant mass consumption in the case of high thrust, low thrust electrical propulsion is considered for the CARINA spacecraft. Therefore, the highly efficient and reliable T6 engines employed for the BepiColombo mission will be used in this mission, with some modifications taking into account probable technological improvement during mission development. Its characteristics are the following: a thrust level of $0.2\,N$, a specific impulse of $I_{sp} = 4000$ s, a power of $4.0\,kW$ and a diameter of $22\,cm$. The system mass is considered equal to $138.8\,kg$; this value is taken from [102] by considering an array of 4 thrusters, with only 2 thrusting at the same time, and 2 propulsion power units in order to obtain the maximum reliability.

5.3. Communication and data handling

The telecommunication subsystem is responsible for providing the spacecraft with the ability to receive, detect and process the telecommand (uplink), as well as performing range and range rate measurements, telemetry modulation and transmission. The system operates in X-band during the uplink and in X- or Ka-band ($8.2\,GHz$, $18\,GHz$) during the telemetry (downlink). One high-gain antenna will be used for scientific data (highly demanding phase), telemetry, and housekeeping in X- or Ka-band during downlink and one medium-gain antenna will be used during up/downlink in the X-band for long-distance telemetry, housekeeping, and emergency far from Earth. Furthermore, two low-gain antennas operating in the S-band will be used for emergencies, redundancy, and omnidirectional communication close to Earth. Three of ESA's deep space ground stations are chosen as the ground stations (CEB1, NNO1, MLG1) [103]. A data rate of $60\,kbit/s$ and $300\,kbit/s$ with a transmission power of $170\,W$ and $125\,W$ respectively using a high-gain antenna diameter of $1.7\,m$ and a ground receive antenna diameter of $35\,m$ has been used as input parameters in the downlink budget. According to the budget, the system is capable of delivering a transmission data rate of 822 kilobits per second and 151 kilobits per second, respectively, for the inputs mentioned above.

Table 7
AOCS devices.

Sensors/Actuators	Performances	TRL
Start tracker [104] (2×)	Accuracy: 4.5 arcsec (xy-plane)	9
	36 arcsec (z-axis)	
Gyro [104] (1×)	Angle Random Walk: $0.01 \deg/\sqrt{hr}$	9
Laser Range [104]	Range: 1 km	9
	Accuracy: 0.5 m	
Reaction wheels [105] (4×)	Angular Momentum: 12 Nms	9
	Torque: 75 mN m	
Hydrazine Thrusters [106] (2 × 8)	Maximum Thrust: 20 N	9
	I_{sp}: 230 s	

Table 8
Budget with a system 20% margin. Component margins are accounted within each subsystem.

Item	Mass (kg)
Data handling	14.70
Communication	102.80
Thermal	52.16
AOCS/GNC	34.86
Power	136.50
Propulsion	229.74
Mechanism/Structure	119.59
Landing Legs	26.88
Harness	44.56
Payload	86.89
ERC	35.64
Nominal Dry Mass at Launch	848.67
Total Dry Mass at Launch	**1018.40**
Total Wet Mass at Launch	**1756.65**

5.4. Thermal design

The thermal system is designed to fulfil the temperature requirements of the different spacecraft components. By considering the spacecraft as consisting of two nodes, main body and solar panels, a model was derived to calculate the spacecraft temperature during the different mission phases similar to other deep space missions [107]. In the cruise phases, the solar radiation and the internal heat dissipation will be the dominating heat sources affecting the spacecraft. In the vicinity of the asteroid, the albedo radiation is taken into account as well. During each phase an average distance from the Sun is assumed. Using a combination of passive and active thermal control systems it will be possible to keep the overall spacecraft temperature within 272–314 K. The total radiator size will be $3.5\,m^2$, covered with louvres to adjust thermal radiation to space. In addition, a heater system with a total of 290 W will ensure that the sample to be returned is stored at a constant temperature and that key systems maintain their operational temperature.

5.5. Earth return capsule

A crushable Earth Return Capsule (ERC) would be used to retrieve the surface and subsurface samples from 2002 AT4, according to the guidelines for an unrestricted body classification [108]. The proposed capsule, with a mass of 35.65 kg and diameter of 0.89 m, would perform a direct impact on the ground without the use of a parachute. This impact preference was chosen as there have been numerous studies and testing performed in the past decade [109–111] showing high reliability compared to other parachute retrieval options without considerable mass increase. Therefore, although the planetary protection policy applied here is not as critical as for bodies under class V regulations, the reduced system complexity, low flight time enabling quick retrieval and higher reliability make this recovery option considerably more attractive.

Carvalho et al. [111] refer to the continuous work being performed to improve the TRL of these capsules. At the time of this proposal, a TRL of 4 can be assumed. The capsule shape (60° half-angle sphere-cone forebody) with a low centre of gravity experiences adequate stability margins during re-entry, allowing for a lower spin rate of 2 rpm provided by the spacecraft prior to re-entry [112]. This configuration was studied in previous Mars and asteroid sample return mission proposals such as Marco Polo [113]. Additionally, the payload bay can transport up to 860 g, enclosed in a container of approximately 2.85 kg. The capsule thermal protective system would use phenolic-impregnated carbon ablator (PICA) heatshield material and would have an additional crushable thermal protective structure composed of polymethacrylimide foam and cork material [111].

Recovery equipment would be included, in order to localise the ERC in a short time-frame of 2 h enabling a quick access to the samples. This recovery time baseline was used in numerical simulations performed by Carvalho et al. [111] showing temperatures lower than −10 °C during re-entry and after impact for the payload container. This is critical to keep the chemical integrity of the retrieved samples, namely to preserve volatiles.

5.6. Mass budget

The mass budget accounting for all spacecraft components, the ERC and the propellant is shown in Table 8.

6. Sample curation

CARINA is a Category V mission under "unrestricted" Earth return requirements as defined by Committee on Space Research (COSPAR) Planetary Protection Policy [114] based on the target and mission type — asteroid and sample return with touch-and-go sampling. Since there is no potential biological contamination of both the target body and the Earth, there are no special planetary protection requirements for the sample containment. However, if on one hand there are no biohazard concerns, on the other hand, the chemical entity of the samples must be preserved and protected against a range of contaminants (in particular organics) which may affect the scientific analysis to be conducted on Earth and consequently the mission scientific goals. Recently, Chan et al. [115] addressed the concerns of organic contamination in a comprehensive review, listing potential sources of contamination, and highlighting the fact that terrestrial organic contamination cannot be avoided, only identified, monitored and kept under control.

The collected samples would be stored in the sealed re-entry capsule compartments until it reaches Earth. Contamination control protocols have to be applied to the sampling tools and return capsule and may include precision cleaning techniques with isopropanol and methanol/dichloromethane under ultrasonic conditions. Samples would be retrieved and brought to the European Extra-terrestrial Sample Curation Facility (ESCF) [116], currently under study through the European Curation of Astromaterials Returned from the Exploration of Space (EURO-CARES) project. It would be transferred via refrigerated transport at temperatures below 10 °C, to prevent the loss of intrinsic volatile species. CARINA would be able to learn from the experience of Stardust [117], Hayabusa2 [118], and OSIRIS-REx [99] on contamination evaluation, control, and mitigation for all the mission phases. A fraction of the collected samples is expected to be internationally distributed for initial analysis [116], the rest will be preserved in high-vacuum conditions for future investigations.

7. Conclusions

In this paper, we have introduced CARINA, a space mission concept to the D-type NEA 2002 AT4. We discussed how primitive asteroids, including D-types, are essential targets of future space missions. CARINA aims to return a piece of a D-type asteroid from the near-Earth region, providing high-value science return with low implementation risk. This sample return mission would bring us material not yet present in our meteorite collection and the possibility to study in more detail questions related to the origin of life, the evolution of the Solar System, and the relationship between comets and asteroids.

Declaration of competing interest

No conflict of interest exists. We wish to confirm that there are no known conflicts of interest associated with this publication and there has been no significant financial support for this work that could have influenced its outcome.

Data availability

Data Availability Statement: Data supporting the results reported in this work can be found in the NASA/JPL Small-Body Database (https://ssd.jpl.nasa.gov/tools/sbdb_lookup.html, last access on 26 January 2023).

Acknowledgements

References

[1] A. Fujiwara, J. Kawaguchi, D. Yeomans, M. Abe, T. Mukai, T. Okada, J. Saito, H. Yano, M. Yoshikawa, D. Scheeres, et al., The rubble-pile asteroid itokawa as observed by hayabusa, Science 312 (5778) (2006) 1330–1334.

[2] S.-i. Watanabe, Y. Tsuda, M. Yoshikawa, S. Tanaka, T. Saiki, S. Nakazawa, Hayabusa2 mission overview, Space Sci. Rev. 208 (1) (2017) 3–16.

[3] D. Lauretta, S. Balram-Knutson, E. Beshore, W. Boynton, C.D. d'Aubigny, D. DellaGiustina, H. Enos, D. Golish, C. Hergenrother, E. Howell, et al., OSIRIS-REx: sample return from asteroid (101955) Bennu, Space Sci. Rev. 212 (1) (2017) 925–984.

[4] D.J. Tholen, Asteroid taxonomy from cluster analysis of photometry, The University of Arizona, 1984.

[5] F.E. DeMeo, R.P. Binzel, S.M. Slivan, S.J. Bus, An extension of the bus asteroid taxonomy into the near-infrared, Icarus 202 (1) (2009) 160–180.

[6] J. Gradie, J. Veverka, The composition of the trojan asteroids, Nature 283 (5750) (1980) 840–842.

[7] D.P. Cruikshank, Organic matter in the outer solar system: From the meteorites to the kuiper belt, in: From Stardust To Planetesimals, vol. 122, 1997, p. 315.

[8] W.K. Hartmann, D.J. Tholen, D.P. Cruikshank, The relationship of active comets, "extinct" comets, and dark asteroids, Icarus 69 (1) (1987) 33–50.

[9] F. Roig, A. Ribeiro, R. Gil-Hutton, Taxonomy of asteroid families among the jupiter trojans: comparison between spectroscopic data and the sloan digital sky survey colors, Astron. Astrophys. 483 (3) (2008) 911–931.

[10] F.E. DeMeo, B. Carry, Solar system evolution from compositional mapping of the asteroid belt, Nature 505 (7485) (2014) 629–634.

[11] R. Binzel, F. DeMeo, E. Turtelboom, S. Bus, A. Tokunaga, T. Burbine, C. Lantz, D. Polishook, B. Carry, A. Morbidelli, et al., Compositional distributions and evolutionary processes for the near-earth object population: Results from the MIT-hawaii near-earth object spectroscopic survey (MITHNEOS), Icarus 324 (2019) 41–76.

[12] T. Hiroi, M.E. Zolensky, C.M. Pieters, The tagish lake meteorite: A possible sample from a D-type asteroid, Science 293 (5538) (2001) 2234–2236.

[13] A.R. Hildebrand, P.J. McCausland, P.G. Brown, F.J. Longstaffe, S.D. Russell, E. Tagliaferri, J.F. Wacker, M.J. Mazur, The fall and recovery of the tagish lake meteorite, Meteorit. Planet. Sci. 41 (3) (2006) 407–431.

[14] P. Vernazza, R. Fulvio, R. Brunetto, J. Emery, C. Dukes, F. Cipriani, O. Witasse, M. Schaible, B. Zanda, G. Strazzulla, et al., Paucity of tagish lake-like parent bodies in the asteroid belt and among jupiter trojans, Icarus 225 (1) (2013) 517–525.

[15] G.M. Gartrelle, P.S. Hardersen, M.R. Izawa, M.C. Nowinski, Round up the unusual suspects: Near-earth asteroid 17274 (2000 LC16) a plausible D-type parent body of the tagish lake meteorite, Icarus 361 (2021) 114349.

[16] B. Yang, D. Jewitt, Spectroscopic search for water ice on Jovian Trojan asteroids, Astron. J. 134 (1) (2007) 223.

[17] J.M. Bauer, T.L. Roush, T.R. Geballe, K.J. Meech, T.C. Owen, W.D. Vacca, J.T. Rayner, K.T. Jim, The near infrared spectrum of miranda: Evidence of crystalline water ice, Icarus 158 (1) (2002) 178–190.

[18] J.P. Emery, R. Brown, Constraints on the surface composition of trojan asteroids from near-infrared (0.8–4.0 μm) spectroscopy, Icarus 164 (1) (2003) 104–121.

[19] T. Noguchi, T. Matsumoto, A. Miyake, Y. Igami, M. Haruta, H. Saito, S. Hata, Y. Seto, M. Miyahara, N. Tomioka, et al., A dehydrated space-weathered skin cloaking the hydrated interior of ryugu, Nat. Astron. (2022) 1–12.

[20] W. Fujiya, P. Hoppe, T. Ushikubo, K. Fukuda, P. Lindgren, M.R. Lee, M. Koike, K. Shirai, Y. Sano, Migration of D-type asteroids from the outer solar system inferred from carbonate in meteorites, Nat. Astron. 3 (10) (2019) 910–915.

[21] H.F. Levison, W.F. Bottke, M. Gounelle, A. Morbidelli, D. Nesvornỳ, K. Tsiganis, Contamination of the asteroid belt by primordial trans-neptunian objects, Nature 460 (7253) (2009) 364–366.

[22] T. Ribeiro, D. Athanasopoulos, H. Bates, E. Bratli, M.J. Breedveld, A. D'Ambrosio, G. Calabuig, O. Gassot, S.-B. Gerig, J.L. Gómez-González, et al., CARINA: A sample return mission concept to a near-earth D-type asteroid, EPSC 2019 (2019) EPSC–DPS2019.

[23] Y.R. Fernández, D.C. Jewitt, S.S. Sheppard, Albedos of asteroids in comet-like orbits, Astron. J. 130 (1) (2005) 308.

[24] D. Jewitt, The active asteroids, Astron. J. 143 (3) (2012) 66.

[25] C. Hergenrother, C. Adam, P. Antreasian, M. Al Asad, S. Balram-Knutson, R. Ballouz, A. Bartels, M.A. Barucci, K. Becker, P. Bland, et al., (101955) Bennu is an active asteroid, EPSC 2019 (2019) EPSC–DPS2019.

[26] M. Gounelle, The asteroid-comet continuum: In search of lost primitivity, Elements 7 (1) (2011) 29–34.

[27] H.H. Hsieh, Asteroid–comet continuum objects in the solar system, Phil. Trans. R. Soc. A 375 (2097) (2017) 20160259.

[28] M.A. Barucci, P. Michel, Asteroid-comet continuum: no doubt but many questions, in: EPSC-DPS Joint Meeting 2019, Vol. 2019, 2019, pp. EPSC–DPS2019.

[29] E.J. Öpik, The stray bodies in the solar system. Part I. Survival of cometary nuclei and the asteroids, Adv. Astron. Astrophys 2 (1963) 219–262.

[30] B. Marsden, On the relationship between comets and minor planets, in: Periodic Orbits, Stability and Resonances, Springer, 1970, pp. 151–163.

[31] M. Hicks, B. Buratti, R. Newburn Jr., D. Rabinowitz, Physical observations of 1996 PW and 1997 SE5: Extinct comets or D-type asteroids? Icarus 143 (2) (2000) 354–359.

[32] M. Mommert, J.L. Hora, A.W. Harris, W.T. Reach, J.P. Emery, C.A. Thomas, M. Mueller, D.P. Cruikshank, D.E. Trilling, M. Delbo, et al., The discovery of cometary activity in near-earth asteroid (3552) don quixote, Astrophys. J. 781 (1) (2014) 25.

[33] D. Lauretta, C. Hergenrother, S. Chesley, J. Leonard, J. Pelgrift, C. Adam, M. Al Asad, P. Antreasian, R.-L. Ballouz, K. Becker, et al., Episodes of particle ejection from the surface of the active asteroid (101955) bennu, Science 366 (6470) (2019) eaay3544.

[34] C. Hergenrother, C. Adam, S. Chesley, D. Lauretta, Introduction to the special issue: exploration of the activity of asteroid (101955) bennu, J. Geophysical Research: Planets 125 (9) (2020) e2020JE006549.

[35] J.L. Molaro, C.W. Hergenrother, S. Chesley, K.J. Walsh, R.D. Hanna, C.W. Haberle, S.R. Schwartz, R.-L. Ballouz, W. Bottke, H. Campins, et al., Thermal fatigue as a driving mechanism for activity on asteroid bennu, J. Geophys.l Res. Planets 125 (8) (2020) e2019JE006325.

[36] R.P. Binzel, A.S. Rivkin, J.S. Stuart, A.W. Harris, S.J. Bus, T.H. Burbine, Observed spectral properties of near-earth objects: results for population distribution, source regions, and space weathering processes, Icarus 170 (2) (2004) 259–294.

[37] F. DeMeo, R.P. Binzel, Comets in the near-earth object population, Icarus 194 (2) (2008) 436–449.

[38] P.R. Weissman, M.F. A'Hearn, L. McFadden, H. Rickman, Evolution of comets into asteroids, Asteroids III 1 (2002) 669.

[39] D. Brownlee, P. Tsou, J. Anderson, M. Hanner, R. Newburn, Z. Sekanina, B. Clark, F. Hörz, M. Zolensky, J. Kissel, et al., Stardust: Comet and interstellar dust sample return mission, J. Geophys. Res. Planets 108 (E10) (2003).

[40] K.-H. Glassmeier, H. Boehnhardt, D. Koschny, E. Kührt, I. Richter, The rosetta mission: flying towards the origin of the solar system, Space Sci. Rev. 128 (1) (2007) 1–21.

[41] M. Barucci, M. Fulchignoni, Major achievements of the rosetta mission in connection with the origin of the solar system, Astron. Astrophys. Rev. 25 (1) (2017) 1–52.

[42] C. Snodgrass, G.H. Jones, The European space agency's comet interceptor lies in wait, Nat. Commun. 10 (1) (2019) 1–4.

[43] M.A. Sephton, Organic compounds in carbonaceous meteorites, Nat. Prod. Rep. 19 (3) (2002) 292–311.

[44] R.M. Flügel, Chirality and Life: A Short Introduction To the Early Phases of Chemical Evolution, Springer Science & Business Media, 2011.

[45] D.P. Glavin, J.P. Dworkin, Enrichment of the amino acid L-isovaline by aqueous alteration on ci and CM meteorite parent bodies, Proc. Natl. Acad. Sci. 106 (14) (2009) 5487–5492.

[46] I. Myrgorodska, C. Meinert, Z. Martins, L. Le Sergeant d'Hendecourt, U.J. Meierhenrich, Molecular chirality in meteorites and interstellar ices, and the chirality experiment on board the ESA cometary rosetta mission, Angew. Chem., Int. Ed. Engl. 54 (5) (2015) 1402–1412.

[47] S.N. Raymond, T. Quinn, J.I. Lunine, Making other earths: dynamical simulations of terrestrial planet formation and water delivery, Icarus 168 (1) (2004) 1–17.

[48] K. Altwegg, H. Balsiger, A. Bar-Nun, J.-J. Berthelier, A. Bieler, P. Bochsler, C. Briois, U. Calmonte, M. Combi, J. De Keyser, et al., 67P/churyumov-gerasimenko, a jupiter family comet with a high D/H ratio, Science 347 (6220) (2015) 1261952.

[49] A. Morbidelli, J. Chambers, J. Lunine, J.-M. Petit, F. Robert, G.B. Valsecchi, K. Cyr, Source regions and timescales for the delivery of water to the earth, Meteorit. Planet. Sci. 35 (6) (2000) 1309–1320.

[50] F. Robert, The D/H ratio in chondrites, Space Sci. Rev. 106 (1–4) (2003) 87–101.

[51] C.M.O. Alexander, The origin of inner solar system water, Phil. Trans. R. Soc. A 375 (2094) (2017) 20150384.

[52] Y. Marrocchi, L. Piani, The tumultuous childhood of the solar system, Nat. Astron. 3 (10) (2019) 889–890.

[53] K. Tsiganis, R. Gomes, A. Morbidelli, H.F. Levison, Origin of the orbital architecture of the giant planets of the solar system, Nature 435 (7041) (2005) 459–461.

[54] F.E. DeMeo, R.P. Binzel, B. Carry, D. Polishook, N.A. Moskovitz, Unexpected D-type interlopers in the inner main belt, Icarus 229 (2014) 392–399.

[55] F. DeMeo, C. Alexander, K. Walsh, C. Chapman, R. Binzel, The compositional structure of the asteroid belt, Asteroids iv 1 (2015) 13.

[56] D. Vokrouhlický, W.F. Bottke, D. Nesvorný, Capture of trans-neptunian planetesimals in the main asteroid belt, Astron. J. 152 (2) (2016) 39.

[57] M.A. Barucci, D. Perna, M. Popescu, S. Fornasier, A. Doressoundiram, C. Lantz, F. Merlin, M. Fulchignoni, E. Dotto, S. Kanuchova, Small D-type asteroids in the NEO population: new targets for space missions, Mon. Not. R. Astron. Soc. 476 (4) (2018) 4481–4487.

[58] M. Yamanobe, T. Nakamura, D. Nakashima, Oxygen isotope reservoirs in the outer asteroid belt inferred from oxygen isotope systematics of chondrule olivines and isolated forsterite and olivine grains in tagish lake-type carbonaceous chondrites, WIS 91600 and MET 00432, Polar Sci. 15 (2018) 29–38.

[59] Y. Marrocchi, G. Avice, J.-A. Barrat, The tarda meteorite: A window into the formation of D-type asteroids, Astrophys. J. Lett. 913 (1) (2021) L9.

[60] J.M. Friedrich, M.-S. Wang, M.E. Lipschutz, Comparison of the trace element composition of tagish lake with other primitive carbonaceous chondrites, Meteorit. Planet. Sci. 37 (5) (2002) 677–686.

[61] M. Zolensky, K. Nakamura, M. Gounelle, T. Mikouchi, T. Kasama, O. Tachikawa, E. Tonui, Mineralogy of tagish lake: An ungrouped type 2 carbonaceous chondrite, Meteorit. Planet. Sci. 37 (5) (2002) 737–761.

[62] G. Consolmagno, D. Britt, R. Macke, The significance of meteorite density and porosity, Geochemistry 68 (1) (2008) 1–29.

[63] P.G. Brown, A.R. Hildebrand, M.E. Zolensky, M. Grady, R.N. Clayton, T.K. Mayeda, E. Tagliaferri, R. Spalding, N.D. MacRae, E.L. Hoffman, et al., The fall, recovery, orbit, and composition of the tagish lake meteorite: A new type of carbonaceous chondrite, Science 290 (5490) (2000) 320–325.

[64] H.F. Levison, C.B. Olkin, K.S. Noll, S. Marchi, J.F. Bell III, E. Bierhaus, R. Binzel, W. Bottke, D. Britt, M. Brown, et al., Lucy mission to the trojan asteroids: Science goals, Planet. Sci. J. 2 (5) (2021) 171.

[65] R.P. Binzel, E. Perozzi, A.S. Rivkin, A. Rossi, A.W. Harris, S.J. Bus, G.B. Valsecchi, S.M. Slivan, Dynamical and compositional assessment of near-earth object mission targets, Meteorit. Planet. Sci. 39 (3) (2004) 351–366.

[66] P. Michel, M. Delbo, Orbital and thermal evolutions of four potential targets for a sample return space mission to a primitive near-earth asteroid, Icarus 209 (2) (2010) 520–534.

[67] I. Carnelli, A. Gàlvez, D. Izzo, Don quijote: A NEO deflection precursor mission, in: NASA Workshop: Near-Earth Object Detection, Characterization, and Threat Mitigation, Citeseer, 2006.

[68] B.D. Warner, A.W. Harris, P. Pravec, The asteroid lightcurve database, Icarus 202 (1) (2009) 134–146.

[69] M. Delbó, A.W. Harris, Physical properties of near-earth asteroids from thermal infrared observations and thermal modeling, Meteorit. Planet. Sci. 37 (12) (2002) 1929–1936.

[70] R. Dymock, The H and G magnitude system for asteroids, J. Br. Astron. Assoc. 117 (2007) 342–343.

[71] A. Fitzsimmons, M. Dahlgren, C.-I. Lagerkvist, P. Magnusson, I. Williams, A spectroscopic survey of D-type asteroids, Astron. Astrophys. 282 (1994) 634–642.

[72] J.R. Spencer, L.A. Lebofsky, M.V. Sykes, Systematic biases in radiometric diameter determinations, Icarus 78 (2) (1989) 337–354.

[73] J.R. Spencer, A rough-surface thermophysical model for airless planets, Icarus 83 (1) (1990) 27–38.

[74] W.F. Bottke Jr., A. Cellino, P. Paolicchi, R.P. Binzel, An overview of the asteroids: the asteroids III perspective, Asteroids III 1 (2002) 3–15.

[75] A. Hérique, B. Agnus, E. Asphaug, A. Barucci, P. Beck, J. Bellerose, J. Biele, L. Bonal, P. Bousquet, L. Bruzzone, et al., Direct observations of asteroid interior and regolith structure: science measurement requirements, Adv. Space Res. 62 (8) (2018) 2141–2162.

[76] C. Opeil, G. Consolmagno, D. Britt, The thermal conductivity of meteorites: New measurements and analysis, Icarus 208 (1) (2010) 449–454.

[77] K. Yomogida, T. Matsui, Physical properties of ordinary chondrites, J. Geophys. Research: Solid Earth 88 (B11) (1983) 9513–9533.

[78] C. Xie, Interactive heat transfer simulations for everyone, Phys. Teach. 50 (4) (2012) 237–240.

[79] W. Fujiya, N. Sugiura, Y. Sano, H. Hiyagon, Mn–cr ages of dolomites in CI chondrites and the tagish lake ungrouped carbonaceous chondrite, Earth Plan. Sci. Lett. 362 (2013) 130–142.

[80] F. Low, D. Beintema, T. Gautier, F. Gillett, C. Beichman, G. Neugebauer, E. Young, H. Aumann, N. Boggess, J. Emerson, et al., Infrared cirrus-new components of the extended infrared emission, Astrophys. J. 278 (1984) L19–L22.

[81] H.U. Keller, C. Barbieri, P. Lamy, H. Rickman, R. Rodrigo, K.-P. Wenzel, H. Sierks, M.F. A'Hearn, F. Angrilli, M. Angulo, et al., OSIRIS–the scientific camera system onboard rosetta, Space Sci. Rev. 128 (2007) 433–506.

[82] M.A. Barucci, A. Cheng, P. Michel, L. Benner, R. Binzel, P. Bland, H. Böhnhardt, J. Brucato, A.C. Bagatin, P. Cerroni, et al., MarcoPolo-R near earth asteroid sample return mission, Exp. Astron. 33 (2–3) (2012) 645–684.

[83] J.-L. Josset, A. Souchon, M. Josset, I. Leya, M. Barucci, S. Fornasier, P. Michel, H. Hoffmann, N. Schmitz, et al., The close-up camera of the marco-polo-r asteroid mission, science objectives and description, in: European Planetary Science Congress, 2013, EPSC2013–1085.

[84] T. Iwata, K. Kitazato, M. Abe, M. Ohtake, T. Arai, T. Arai, N. Hirata, T. Hiroi, C. Honda, N. Imae, et al., NIRS3: the near infrared spectrometer on Hayabusa2, Space Sci. Rev. 208 (1) (2017) 317–337.

[85] F. Poulet, C. Gomez, J.-P. Bibring, Y. Langevin, B. Gondet, P. Pinet, G. Belluci, J. Mustard, Martian surface mineralogy from observatoire pour la minéralogie, l'eau, les glaces et l'activité on board the mars express spacecraft (OMEGA/MEx): global mineral maps, J. Geophys. Res. Planets 112 (E8) (2007).

[86] N. Bowles, C. Snodgrass, A. Gibbings, J.-P. Sanchez, J. Arnold, P. Eccleston, T. Andert, A. Probst, G. Naletto, A. Vandaele, et al., CASTAway: An asteroid main belt tour and survey, Adv. Space Res. 62 (8) (2018) 1998–2025.

[87] C. Snodgrass, G.H. Jones, H. Böhnhardt, A. Gibbings, M. Homeister, N. Andre, P. Beck, M. Bentley, I. Bertini, N. Bowles, et al., The castalia mission to main belt comet 133P/Elst-Pizarro, Adv. Space Res. 62 (8) (2018) 1947–1976.

[88] I. Wright, S. Barber, G. Morgan, A. Morse, S. Sheridan, D. Andrews, J. Maynard, D. Yau, S. Evans, M. Leese, et al., Ptolemy–an instrument to measure stable isotopic ratios of key volatiles on a cometary nucleus, Space Sci. Rev. 128 (2007) 363–381.

[89] J.F. Todd, S.J. Barber, I.P. Wright, G.H. Morgan, A.D. Morse, S. Sheridan, M.R. Leese, J. Maynard, S.T. Evans, C.T. Pillinger, et al., Ion trap mass spectrometry on a comet nucleus: the ptolemy instrument and the rosetta space mission, J Mass Spectrom. 42 (1) (2007) 1–10.

[90] A. Hérique, D. Plettemeier, C. Lange, J.T. Grundmann, V. Ciarletti, T.-M. Ho, W. Kofman, B. Agnus, J. Du, W. Fa, et al., A radar package for asteroid subsurface investigations: Implications of implementing and integration into the MASCOT nanoscale landing platform from science requirements to baseline design, Acta Astronaut. 156 (2019) 317–329.

[91] D. Herčík, H.-U. Auster, J. Blum, K.-H. Fornaçon, M. Fujimoto, K. Gebauer, C. Güttler, O. Hillenmaier, A. Hördt, E. Liebert, et al., The MASCOT magnetometer, Space Sci. Rev. 208 (2017) 433–449.

[92] D. Mihai, R. Mihalache, G. Megherelu, E. Nutu, I.F. Popa, M. Sima, A. Adiaconitei, E.C. Paul, Design and testing of a closing and sealing system for a phobos sample return mission, Adv. Space Res. 69 (2) (2022) 1170–1197.

[93] S. Völk, S. Ulamec, J. Biele, M. Hecht, P. Lell, J. Fleischmann, S. Althapp, M. Grebenstein, J.A. Nuth, D.C. Wegel, et al., Development and testing of a pyro-driven launcher for harpoon-based comet sample acquisition, Acta Astronaut. 152 (2018) 218–228.

[94] Ariane 6, 2023, https://www.arianespace.com/ariane-6/. (Accessed 26 January 2023).

[95] F. Biscani, D. Izzo, M. Mrtens, Esa/pagmo2: pagmo 2.7 [online slides], 2018, http://dx.doi.org/10.5281/zenodo.1217831.

[96] P.E. Gill, W. Murray, M.A. Saunders, SNOPT: An SQP algorithm for large-scale constrained optimization, SIAM Rev. 47 (1) (2005) 99–131.

[97] R.M. Pinson, P. Lu, Trajectory design employing convex optimization for landing on irregularly shaped asteroids, J. Guid. Control Dyn. 41 (6) (2018) 1243–1256, http://dx.doi.org/10.2514/1.g003045.

[98] G.J. Dominguez Calabuig, E. Mooij, Optimal on-board abort guidance based on successive convexification for atmospheric re-entry, in: AIAA Scitech 2021 Forum, 2021, p. 0860.

[99] J. Dworkin, L. Adelman, T. Ajluni, A. Andronikov, J. Aponte, A. Bartels, E. Beshore, E. Bierhaus, J. Brucato, B. Bryan, et al., OSIRIS-REx contamination control strategy and implementation, Space Sci. Rev. 214 (2018) 1–53.

[100] A. Ferri, S. Pelle, M. Belluco, T. Voirin, R. Gelmi, The exploration of PHOBOS: Design of a sample return mission, Adv. Space Res. 62 (8) (2018) 2163–2173.

[101] N.X. Vinh, A. Busemann, R.D. Culp, Hypersonic and Planetary Entry Flight Mechanics, University of Michigan Press, 1980.

[102] M. Hutchins, H. Simpson, J. Palencia Jimenez, Qinetiq's T6 and T5 ion thruster electric propulsion system architectures and performances, in: 30th International Symposium on Space Technology and Science, Hyogo-Kobe, Japan, 2015, IEPC-2015-131/ISTS-2015-b-131.

[103] Y. Doat, M. Lanucara, P.-M. Besso, T. Beck, G. Lorenzo, M. Butkowic, ESA tracking network–a European asset, in: 2018 SpaceOps Conference, 2018, p. 2306.

[104] Jena-optronik, 2023, https://www.jena-optronik.de/en/home.html. (Accessed 26 January 2023).

[105] Collins aerospace, 2023, https://www.rockwellcollins.com/Products-and-Services/Defense/Platforms/Space.aspx. (Accessed 26 January 2023).

[106] Ariane's 20N thruster, 2023, https://www.ariane.group/en/equipment-and-services/satellites-and-spacecraft/20n/. (Accessed 26 January 2023).

[107] J. Meseguer, I. Pérez-Grande, A. Sanz-Andrés, Spacecraft Thermal Control, Elsevier, 2012.

[108] C. Bureau, COSPAR policy on planetary protection, Space Res. Today (208) (2020) 10–12.

[109] S. Kellas, Passive earth entry vehicle landing test, in: Aerospace Conference, 2017 IEEE, IEEE, 2017, pp. 1–10.

[110] T. Yamada, T. Ogasawara, K. Kitazono, H. Tanno, High-speed compact entry capsule enhanced by lightweight ablator and crushable structure, Trans. Japan Soc. Aeronaut. Space Sci. Aerosp. Technol. Japan 14 (ists30) (2016) Pe_33–Pe_40.

[111] J. Carvalho, C. Ribeiro, R. Sa, A. Marques, F. Carneiro, P. Chaves, P. Antunes, D. Rebufatt, I. Ngan, Conceptual design of a crushable thermal protection system for the ERCC, in: Proceedings of the 7th International Conference on Mechanics and Materials in Design, 2017.

[112] P. Desai, R. Mitcheltree, F.M. Cheatwood, Sample returns missions in the coming decade, in: 51st International Astronautical Congress, Rio de Janeiro, Brazil, 2000, IAF-00-Q.2.04.

[113] M.A. Barucci, A.F. Cheng, P. Michel, L.A.M. Benner, R.P. Binzel, P.A. Bland, H. Bohnhardt, MarcoPolo-R near earth asteroid sample return mission, Springer Science + Buisness Media B. V., 2012, http://dx.doi.org/10.1007/s10686-011-9231-8.

[114] J. Rummel, P. Stabekis, D. Devincenzi, J. Barengoltz, COSPAR's planetary protection policy: A consolidated draft, Adv. Space Res. 30 (6) (2002) 1567–1571.

[115] Q.H.S. Chan, R. Stroud, Z. Martins, H. Yabuta, Concerns of organic contamination for sample return space missions, Space Sci. Rev. 216 (2020) 1–40.

[116] S. Russell, C. Smith, A. Hutzler, A. Meneghin, L. Berthoud, J. Aleon, A. Bennett, J. Bridges, J.R. Brucato, V. Debaille, et al., EURO-CARES-a European sample curation facility for sample return missions, in: 2019 IEEE Aerospace Conference, IEEE, 2019, pp. 1–9.

[117] S.A. Sandford, S. Bajt, S.J. Clemett, G.D. Cody, G. Cooper, B.T. Degregorio, V. de Vera, J.P. Dworkin, J.E. Elsila, G.J. Flynn, et al., Assessment and control of organic and other contaminants associated with the stardust sample return from comet 81p/wild 2, Meteorit. Planet. Sci. 45 (3) (2010) 406–433.

[118] F. Kitajima, M. Uesugi, Y. Karouji, Y. Ishibashi, T. Yada, H. Naraoka, M. Abe, A. Fujimura, M. Ito, H. Yabuta, et al., A micro-Raman and infrared study of several hayabusa category 3 (organic) particles, Earth Planets Space 67 (2015) 1–12.